Effect of Volume Fraction on the Order−Disorder Transition in Low Molecular Weight Polystyrene-*block*-polyisoprene Copolymers. 2. Order−Disorder Transition Temperature Determined by Small-Angle X-ray Scattering

Toshihiro Ogawa, Naoki Sakamoto, and Takeji Hashimoto*

Department of Polymer Chemistry, Graduate School of Engineering, Kyoto University, Kyoto 606, Japan

Chang Dae Han and Deog Man Baek†

Department of Polymer Engineering, The University of Akron, Akron, Ohio 44325-0301

Received July 24, 1995; Revised Manuscript Received December 5, 1995⊗

ABSTRACT: Small-angle X-ray scattering (SAXS) was employed to investigate the order−disorder transition of low molecular weight polystyrene-*block*-polyisoprene (SI diblock) copolymers with widely varying composition. The SI diblock copolymers investigated in the present study have molecular weight varying from 15 000 to 41 000 and the volume fraction of PS block varying from 0.186 to 0.811. Low-temperature resolution SAXS experiments, which involved a temperature increment of ≥10 °C, did not allow us to accurately determine the order−disorder transition temperatures (T_{ODT}) of the SI diblock copolymers, but high-temperature resolution SAXS experiments, which involved measurements of the scattering profiles across T_{ODT} with a small temperature increment of ≤1 °C, enabled us to determine the values of T_{ODT} with accuracy to within ±1 °C. T_{ODT} was determined to be the temperature at which the reciprocal of the maximum intensity and the square of the half-width at half-maximum of the first-order scattering maximum change discontinuously with the reciprocal of absolute temperature. We compared the values of T_{ODT} determined from SAXS experiments with those determined from rheological measurements reported in part 1 of this series.

Introduction

In recent years there has been a rather extensive experimental investigation, via small-angle X-ray scattering (SAXS), reported on the order−disorder transition (ODT) of block copolymers. There are too many to cite here, and the interested readers are referred to two recent review articles.[1,2] When reviewing the literature[3−10] which reported on the SAXS measurements of styrene-based block copolymers, specifically polystyrene-*block*-polyisoprene (SI diblock) and polystyrene-*block*-polybutadiene (SB diblock) copolymers, we find that the temperature resolution employed in some SAXS experiments[3,5,9,10] was *not* sufficiently high, and thus accurate determination of order−disorder transition temperatures (T_{ODT}) was difficult, if not impossible. As pointed out in our previous paper,[11] accurate determination of T_{ODT} via SAXS of low molecular weight SI diblock copolymers requires *high-temperature resolution* scattering experiments. The same will equally be applicable to low molecular weight SB diblock copolymers.

In a recent paper[12] we discussed the results of our rheological investigation on the ODT of low molecular weight SI diblock copolymers, which were synthesized in our laboratory. In the present study, by employing the same block copolymers, we continued our investigation on their ODTs using SAXS. The primary purpose of this study was to compare the values of T_{ODT} obtained from SAXS measurements with those obtained previously from rheological measurements.[12] In this paper, as a sequel of the series, we shall report on the highlights of our SAXS measurements for a series of low molecular weight SI diblock copolymers.

The organization of this paper is as follows. First, we shall present the SAXS profiles obtained for seven SI diblock copolymers synthesized in this study. In doing so, we will discuss the microdomain structures expected from the SAXS profiles and then compare them with those determined independently by transmission electron microscopy (TEM). Next, using the overall SAXS profiles obtained over a wide range of temperatures, we shall discuss the ODT of the SI diblock copolymers. For this, we will use the conventional analyses, namely, (i) plots of the reciprocal of the maximum scattered intensity ($1/I_m$) versus the reciprocal of absolute temperature ($1/T$), (ii) plots of the reciprocal of the scattered intensity ($1/I(q^*)$) at a fixed scattering vector q^* versus $1/T$, where $q^* = (4\pi/\lambda)\sin(\theta^*/2)$, θ^* and λ being the particular scattering angle near the scattering maximum and the wavelength of the incident beam, respectively, and (iii) plots of wavelength (D) of a dominant mode of concentration fluctuations versus $1/T$. Then, we will employ plots of the square of half-width at half-maximum (hwhm) (σ_q^2) of the first-order scattering maximum versus $1/T$, which was first introduced by Stühn et al.[7] and Ehlich et al.[13] Finally, we shall discuss the results of *high-temperature resolution* scattering experiments, which involve measurements of the SAXS scattering profiles across T_{ODT} with a *small* temperature increment (as small as ≤1 °C). We will point out that the SAXS experiments with a *low-temperature resolution* (e.g., a temperature increment of ≥10 °C) may overlook the sharpness of the ODT, leading to inaccurate determination of T_{ODT} of block copolymers.

Experimental Section

In this study, seven SI diblock copolymers were synthesized via anionic polymerization, and they were used to investigate via SAXS their ODTs. The details of the procedures employed

† Present address: Polymer Laboratory, Research Center, Dae Lim Industry Ltd., Science Town, Taejeon 305-343, Korea.

⊗ Abstract published in *Advance ACS Abstracts,* February 1, 1996.

0024-9297/96/2229-2113$12.00/0

Table 1. Molecular Characteristics of the SI Diblock Copolymers Synthesized in This Study

sample code	M_w ($\times 10^{-4}$)	M_n ($\times 10^{-4}$)	M_w/M_n	wt % PS	f_{PS}[a]	morphology
SI-Q	2.80	2.64	1.06	21.2	0.186	PS cylinder
SI-Z	1.93	1.77	1.09	33.6	0.303	PS cylinder
SI-S	1.76	1.66	1.06	40.9	0.372	bicontinuous
SI-X	1.79	1.67	1.07	50.0	0.461	lamella
SI-R	1.50	1.40	1.07	54.5	0.508	lamella
SI-O	2.64	2.49	1.06	78.8	0.760	PI cylinder
SI-L	4.10	3.90	1.05	83.3	0.811	PI cylinder

[a] f_{PS} is the volume fraction of PS block in the SI diblock copolymer at 25 °C, which is defined by $f_{PS} = \nu_{PS}N_{PS}/(\nu_{PS}N_{PS} + \nu_{PI}N_{PI})$, where N_{PS} and N_{PI} are the average degrees of polymerization of the PS and PI blocks, respectively, in the SI diblock copolymer, ν_{PS} is the volume per mole of styrene monomer, and ν_{PI} is the volume per mole of isoprene monomer.

for the synthesis of SI diblock copolymers are described elsewhere.[14] Table 1 gives a summary of the molecular characteristics and the volume fraction of the PS phase in each SI block copolymer synthesized. Nuclear magnetic resonance spectroscopy indicated that the microstructure of polyisoprene had 94 wt % 1,4-linkage, 6 wt % 3,4-linkage, and no detectable amount of 1,2-linkage in the SI diblock copolymers.

Samples were prepared by first dissolving a predetermined amount of SI block copolymer (10 wt %) in toluene in the presence of an antioxidant (irganox 1010; Ciba-Geigy Group) and then slowly evaporating the solvent. The evaporation of solvent was carried out slowly at room temperature for 1 week and then in a vacuum oven at 40 °C for 3 days. The last trace of solvent was removed by drying the samples in a vacuum oven at an elevated temperature by gradually raising the oven temperature to 10 °C above the glass transition temperature of the component PS in each block copolymer. The drying of the samples was continued until there was no further change in weight. Finally, the samples were annealed for 10 h at a temperature which was about 20 °C above the glass transition temperature of the component PS.

SAXS experiments were conducted with an apparatus, described in detail elsewhere,[15] which consisted of a 12-kW rotating-anode X-ray generator, a graphite crystal for incident-beam monochromatization, a 1.5-m camera (0.5 m from the source to the sample and 1.0 m from the sample to the detector), and a one-dimensional position-sensitive proportional counter. The Cu Kα line (0.154 nm) was used. The SAXS profiles were measured in situ as a function of temperature and were corrected for absorption, air scattering, and background scattering arising from thermal diffuse scattering and slit-height and slit-width smearing.[16] The absolute SAXS intensity was obtained using the nickel-foil method.[17]

Results and Discussion

Morphology of the Microdomains of SI Diblock Copolymers Determined from SAXS Profiles. The temperature dependence of SAXS profiles are given in Figure 1 for all the SI diblock copolymers synthesized in this study except for SI-O. The profiles for SI-O are not shown here because they are almost the same as those for SI-L. It should be mentioned that these SAXS profiles were obtained during the slow heating cycle, and the thermal histories of the specimens employed during the SAXS experiment are summarized in Table 2. Note that the SAXS profiles are ones which were desmeared and corrected for air scattering, slit-height and slit-width smearings, and absorption. As will be clarified later, these profiles represent those for the ordered state, except for profiles 4 and 5 for SI-S (Figure 1c) which represent those in the disordered state. From these SAXS profiles, we can deduce the microdomain structure in each block copolymer sample. The following observations are worth noting in Figure 1.

The SAXS profiles for SI-Q in Figure 1a indicate that this block copolymer forms either spherical or hexagonally packed cylindrical microdomains of PS phase in PI matrix, as judged from the positions of higher order scattering maximum at the scattering vectors q of 1 and $\sqrt{3}$ relative to the position of first-order scattering maximum. An independent experiment with TEM suggests that SI-Q has hexagonally packed cylindrical microdomains of PS in PI matrix as shown in Figure 2. The sample preparation condition was described in detail elsewhere.[12] A close look at Figure 1a indicates further that as the temperature is increased, the peak broadens. Although not shown here, the higher order maximum first disappears at temperatures of 99 °C and above in which the system attains the disordered state, and only the first-order peak is clearly seen. A broad peak appearing at $q \equiv q_{mp} = 0.87$ nm^{-1} at temperatures lower than 91 °C in Figure 1a (see the thick arrow on curve 1) is believed to be due to the form factor of isolated particles. Figure 2 shows the TEM for SI-Q ultrathin sectioned and stained with OsO_4.

The average radius (R) of the cylinders can be estimated from q_{mp} by using the following formula,

$$q_{mp}R = 4.98, 8.364, 11.46... \text{ for } p = 1, 2, 3... \quad (1)$$

where p is the order of the maxima from the isolated cylinders. The value of R thus estimated is 5.7 nm. The intercylinder distance (D_0) can be calculated from q_m for the first-order peak by assuming hexagonal packing of the cylinders,

$$D_0 = (4/3)^{1/2}D \quad (2)$$

where D is the Bragg spacing estimated from

$$D = 2\pi/q_m \quad (3)$$

where q_m is the scattering vector at the first-order scattering maximum which exists below and above ODT. The value q_m was directly determined from the peak position of the scattering profile measured at a given direction in q-space. Using eqs 2 and 3, we estimate D_0 to be 24.6 nm and D to be 21.3 nm. Thus the volume fraction of the PS cylinders as estimated from the SAXS data, $f_{PS,SAXS}$, by using the following formula

$$f_{PS,SAXS} = \frac{2\pi}{\sqrt{3}}(R/D_0)^2 \quad (4)$$

is 0.195. The volume fraction of the PS block chain, f_{PS}, can also be calculated from the block copolymer composition and the specific volumes of the PS and PI block chains by assuming that the specific volumes are those for the corresponding pure homopolymer phases. The value of f_{PS} is 0.186 as listed in Table 1, which is very close, within experimental uncertainties, to the value of $f_{PS,SAXS}$.

If we assume that the broad peak at q_{mp} is due to the form factor of the PS spherical microdomains, we can estimate the average radius (R) from

$$q_{mp}R = 5.765, 9.10, 12.3... \text{ for } p = 1, 2, 3... \quad (5)$$

The value of R thus estimated is 6.6 nm. If the spheres are packed in face-centered cubic lattice (fcc) or in body-centered cubic lattice (bcc), the nearest neighbor dis-

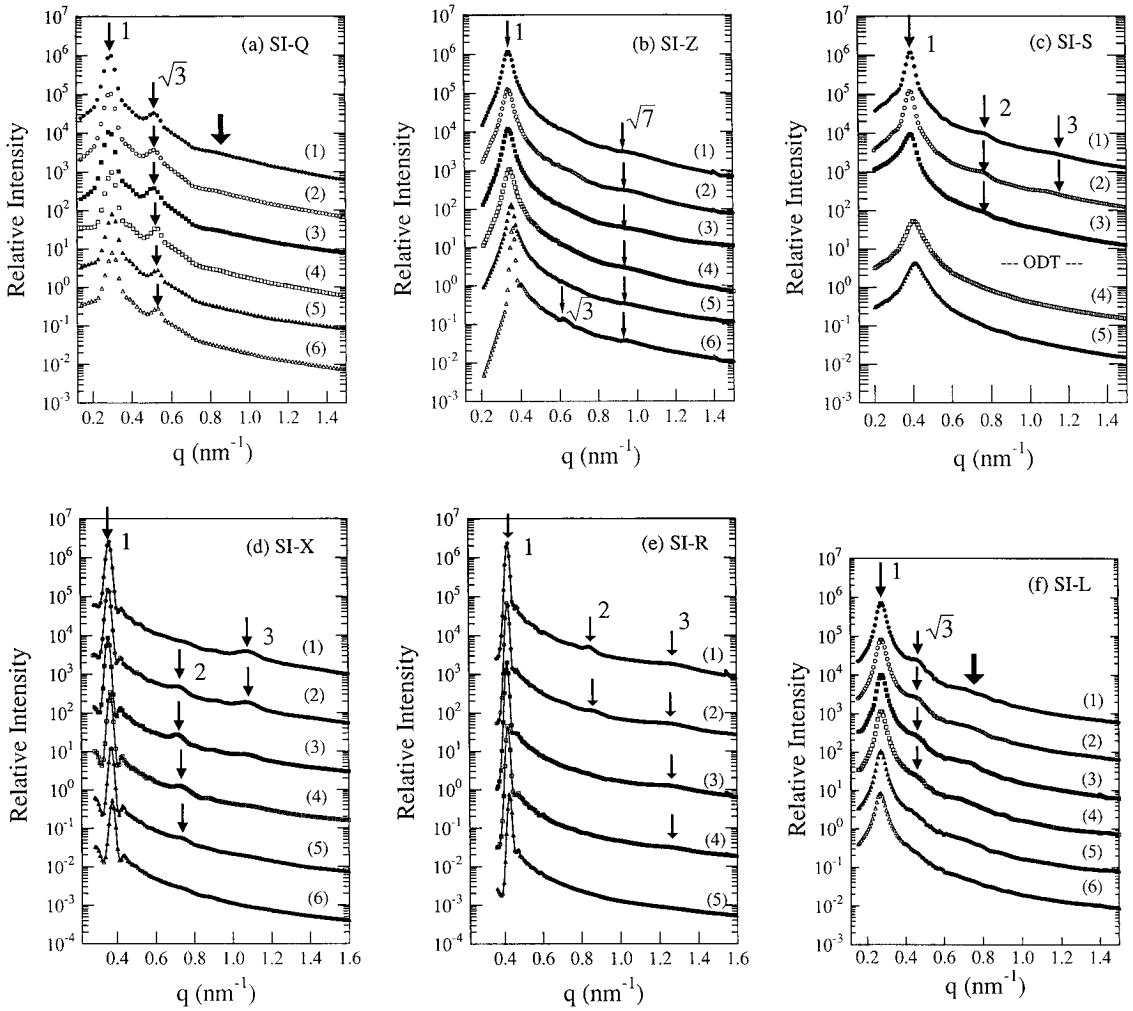

Figure 1. Temperature dependence of the SAXS profiles: (a) SI-Q near the first-order maximum at various temperatures (1) 22, (2) 41, (3) 57, (4) 74, (5) 82, and (6) 91 °C; (b) SI-Z near the first-order maximum at various temperatures (1) 30, (2) 50, (3) 60, (4) 70, (5) 80, and (6) 90 °C; (c) SI-S near the first-order maximum at various temperatures (1) 25, (2) 50, (3) 70, (4) 90, and (5) 100 °C; (d) SI-X near the first-order maximum at various temperatures (1) 25, (2) 50, (3) 70, (4) 90, (5) 100, and (6) 110 °C; (e) SI-R near the first-order maximum at various temperatures (1) 24, (2) 41, (3) 57, (4) 74, and (5) 91; (f) SI-L near the first-order maximum at various temperatures (1) 26, (2) 50, (3) 70, (4) 90, (5) 110, and (6) 130 °C. Each curve in parts a−c and f was shifted by a factor of 10 to avoid overlap, whereas it was shifted by a factor of 20 and 40 in parts d and e, respectively.

tance (D_0) between spheres can be estimated from

$$D_0 = \sqrt{3/2}D \tag{6}$$

where D is the Bragg spacing given by eq 3. The volume fraction of the PS spheres from the SAXS data, $f_{PS,SAXS}$, can be calculated from

$$f_{PS,SAXS} = \frac{4\sqrt{2}}{3}\pi(R/D_0)^3 \tag{7}$$

if the spheres are packed in fcc, or

$$f_{PS,SAXS} = \sqrt{3}\pi(R/D_0)^3 \tag{8}$$

if the spheres are packed in bcc. The value of $f_{PS,SAXS}$ thus estimated is 0.0958 for fcc and 0.0880 for bcc, which are much smaller than $f_{PS} = 0.186$ (see Table 1), indicating that the hexagonal packing of the cylinders is more reasonable than the fcc or bcc spheres. Needless to say, the value of $f_{PS,SAXS}$ becomes even smaller for the spheres in simple cubic lattice than for the spheres in fcc and bcc.

The SAXS profiles for SI-Z in Figure 1b show that as the temperature is increased from 30 to 90 °C the first-order peak becomes sharp, and at 90 °C (profile 6) the higher order scattering maximum appears at the scattering vectors q of 1, $\sqrt{3}$, and $\sqrt{7}$ relative to the position of first-order scattering maximum, indicating that this block copolymer forms hexagonally packed cylindrical microdomains of PS in PI matrix. This observation is consistent with the results of TEM.[12] It should be noted that the sharpening of the first-order peak, observed in Figure 1b,[18] as the temperature increased from 30 to 90 °C is due to the annealing effect.

The SAXS profiles for SI-S in Figure 1c indicate that this block copolymer appears to form lamellar microdomain structure, as judged from the positions of higher order scattering maximum at the scattering vectors q of integer multiples relative to the position of first-order scattering maximum. An independent study from TEM indicates that SI-S does not show well-defined lamellar morphology. TEM tends to show rather bicontinuous microdomains with a considerable distortion, giving the appearance locally of lamellar catenoids.[12] It is not clear at this moment whether or not the bicontinuous structure will show the profiles as shown in Figure 1c. Additional scattering maxima due to the intercatenoidal channels may not necessarily be seen, if their spatial arrangement is considerably distorted. Notice in Figure

Table 2. Thermal History of the Specimen Employed during the SAXS Experiment

sample code	thermal history of the specimen employed during the SAXS experiment[a]
SI-Q	heating began at 22 °C (0 h/0.5 h) → 41 °C (0.5 h/0.5 h) → 57 °C (0.5 h/0.5 h) → 74 °C (0.5 h/0.5 h) → 82 °C (0.5 h/0.83 h) → 91 °C (0.5 h/1 h) → 99 °C (0.5 h/1 h) → 107 °C (0.5 h/1.5 h) → 116 °C (0.5 h/2 h) → 124 °C (0.5 h/2 h) → 132 °C (0.5 h/1 h) → 141 °C (0.5 h/1 h)
SI-Z	heating began at 30 °C (0 h/2 h) → 50 °C (0.5 h/2 h) → 60 °C (2 h/2 h) → 70 °C (0.5 h/2 h) → 80 °C (0.5 h/2 h) → 90 °C (0.5 h/1 h) → 100 °C (0.5 h/1 h) → 110 °C (0.5 h/1 h) → 120 °C (0.5 h/1 h) → 130 °C (0.5 h/1 h) → 140 °C (0.5 h/1 h) → 150 °C (0.5 h/1 h)
SI-S	heating began at 25 °C (0 h/1 h) → 50 °C (0.5 h/1 h) → 70 °C (0.5 h/1 h) → 90 °C (0.5 h/1 h) → 100 °C (0.5 h/1 h) → 110 °C (0.5 h/1 h) → 120 °C (0.5 h/1 h) → 130 °C (0.5 h/1 h) → 140 °C (0.5 h/1 h)
SI-X	heating began at 25 °C (0 h/0.5 h) → 50 °C (0.5 h/0.5 h) → 70 °C (0.5 h/0.5 h) → 90 °C (0.5 h/0.5) → 100 °C (1 h/1 h) → 110 °C (0.5 h/1 h) → 120 °C (0.5 h/1 h) → 130 °C (0.5 h/1 h) → 140 °C (0.5 h/1 h) → 150 °C (0.5 h/1 h) → 160 °C (0.5 h/1 h) → 170 °C (0.5 h/1 h)
SI-R	heating began at 24 °C (0 h/0.67 h) → 41 °C (0.5 h/0.67 h) → 57 °C (0.5 h/0.67 h) → 74 °C (0.5 h/0.67 h) → 91 °C (0.5 h/1.33 h) → 99 °C (0.5 h/1.33 h) → 107 °C (0.5 h/1.33 h) → 116 °C (0.5 h/2 h) → 124 °C (0.5 h/2 h) → 132 °C (0.5 h/2 h) → 141 °C (0.5 h/2.67 h) → 149 °C (0.5 h/2.67 h) → 157 °C (0.5 h/2.67 h)
SI-O	heating began at 30 °C (0 h/2 h) → 60 °C (0.5 h/2 h) → 90 °C (1 h/2 h) → 100 °C (0.6 h/1 h) → 105 °C (0.5 h/1 h) → 110 °C (0.5 h/1 h) → 120 °C (0.5 h/1 h) → 130 °C (0.5 h/1 h) → 135 °C (0.5 h/21 h) → 140 °C (0.5 h/1 h) → 150 °C (0.5 h/1 h) → 160 °C (0.5 h/1 h)
SI-L	heating began at 25 °C (0 h/2 h) → 50 °C (0.5 h/2 h) → 70 °C (0.5 h/2 h) → 90 °C (0.5 h/2 h) → 110 °C (0.5 h/2 h) → 130 °C (0.5 h/2 h) → 150 °C (0.5 h/2 h) → 170 °C (0.5 h/2 h) → 180 °C (0.5 h/2 h) → 190 °C (0.5 h/2 h) → 200 °C (0.5 h/2 h) → 210 °C (0.5 h/4 h)

[a] Inside the parentheses after the temperature, the first number refers to the preheating period before SAXS measurement began and the second number refers to the actual period during which SAXS measurements were taken.

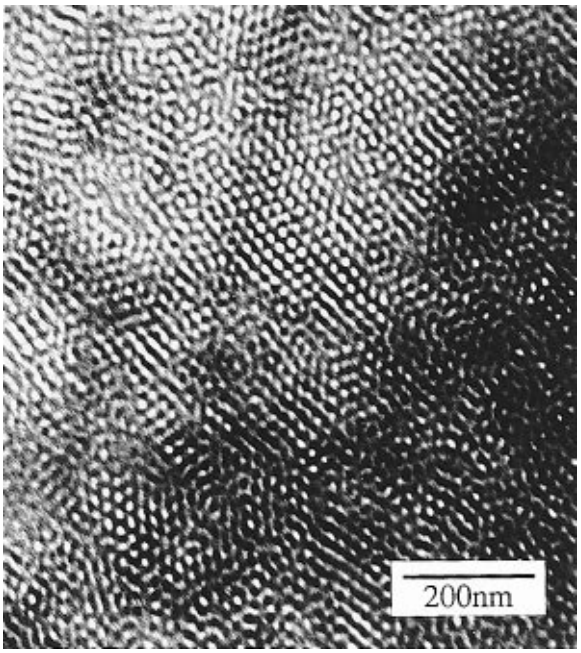

Figure 2. Transmission electron micrograph for SI-Q. The ultrathin sections of ca. 50-nm thickness were obtained by microtoming at −85 °C with a Reichert-Jung Ultracut E instrument together with a cryogenic unit FC4E and a diamond knife. They were picked up on 400-mesh copper grids and then stained by exposure to osmium tetraoxide vapor for a few hours.

1c that the third peak disappears at 70 °C, and only the first-order peak was observed at temperatures of 90 °C and higher (see profiles 4 and 5). The block copolymer is expected to be in the disordered state at the high temperatures as will be clarified later. The detailed SAXS analysis on the microdomain morphology is beyond the scope of the present study and is left for future investigation.

The SAXS profiles for SI-X in Figure 1d[18] indicate that this block copolymer forms lamellar microdomains, as judged from the positions of higher order scattering maximum at the scattering vectors q of integer multiples relative to the position of first-order scattering maximum. An independent study from TEM indicates that SI-X has lamellae in most areas, but in some areas it has imperfect lamellae having the appearance of a distorted, chaotic microdomain morphology.[12] The coexistence of two such regions is believed to be attributable to a nonequilibrium effect on microdomain formation. It should be noted that the scattering peaks in Figure 1d for SI-X are sharper than those in Figure 1c for SI-S, suggesting that the lamellae in SI-X have an order higher than the microdomain structure in SI-S. Notice in Figure 1d that the second scattering peak is missing or weak at 25 °C (profile 1), which is attributable to the fact that the PS and PI lamellae have almost identical volume fractions. The appearance of the second scattering peak at temperatures $50 \leq T \leq 100$ °C is attributable to an offset in the volume fraction of the microdomains from a 50/50 ratio, consistent with the value of $f_{PS} = 0.461$ given in Table 1.

The SAXS profiles for SI-R in Figure 1e[18] indicate that this block copolymer, SI-R, appears to form lamellar microdomains, as judged from the positions of higher order scattering maximum at the scattering vectors q of integer multiples relative to the position of first-order scattering maximum. An independent study from TEM indicates that SI-R has the coexistence of well-developed lamellae and bicontinuous microdomains,[12] which may be attributable to a nonequilibrium effect. The bicontinuous microdomains with the distortion may give rise to only the first-order peak at the scattering vector close to the first-order peak of lamellae. This may be the origin of why we do not observe the two sets of the scattering maxima corresponding to the coexisting morphologies observed in TEM. It is of interest to observe

in Figure 1e that the second scattering peak is suppressed with increasing temperature from 24 to 74 °C, which is believed to be due to the equal volumes of the PS and PI lamellae in SI-R, $f_{PS} = 0.508$ (see Table 1). The annealing effects observed in Figure 1d,e show that the PS lamellae in the as-cast film may have an excess volume, due to vitrification during the solvent evaporation process. This excess volume is relaxed upon annealing. The same argument can be applied to explain the temperature dependence of the second-order peak for SI-X in Figure 1d.

The SAXS profiles for SI-L in Figure 1f indicate that this block copolymer forms either spherical or hexagonally packed cylindrical microdomains of PI in PS matrix, as judged from the positions of higher order scattering maximum at the scattering vectors q of 1 and $\sqrt{3}$ relative to the position of first-order scattering maximum. An independent study with TEM indicates that SI-L has cylindrical microdomains.[12] The broad scattering peak at $q \equiv q_{mp} \cong 0.77$ nm^{-1} appearing in Figure 1f is believed to be due to the form factor of isolated particles.

The average radius (R) of the PI cylinders in SI-L, estimated from eq 1, is 6.5 nm, the intercylinder distance (D_0) estimated from eq 2 is 27.7 nm, and the volume fraction of the PI cylinders, $f_{PI,SAXS}$, estimated from eq 4 (in which $f_{PS,SAXS}$ must be replaced by $f_{PI,SAXS}$), is 0.200. Thus the volume fraction of the PS phase in SI-L can be estimated from $f_{PS,SAXS} = 1 - f_{PI,SAXS}$, yielding $f_{PS,SAXS} = 0.800$, which is very close to $f_{PS} = 0.811$ on the basis of the block copolymer composition (see Table 1). In reference to Figure 1f, if the broad scattering maximum at q_{mp} is assumed to have the origin in the form factor of the PI spheres, (i) R estimated from eq 5 is 7.5 nm, (ii) D_0 in the bcc or fcc lattice estimated from eq 6 is 28.5 nm, and (iii) $f_{PI,SAXS}$ calculated from eqs 7 and 8 is 0.0983 and 0.0903 for fcc and bcc, respectively. Thus $f_{PS,SAXS} = 0.902$ for fcc and 0.910 for bcc, which are much larger than $f_{PS} = 0.811$. Thus we conclude that the hexagonally packed cylindrical microdomains in SI-L are more likely than the spherical microdomains in the cubic symmetries.

Conventional Analyses of SAXS Profiles for Determination of T_{ODT}. There are three different ways, based on mean-field theory, of analyzing SAXS experimental results to investigate the ODT of block copolymers. They are use of the plot of (i) the reciprocal of the maximum scattered intensity ($1/I_m$) versus the reciprocal of absolute temperature ($1/T$), (ii) the reciprocal of the scattered intensity ($1/I(q^*)$) at a fixed scattering vector q^* versus $1/T$, and (iii) wavelength (D) of a dominant mode of concentration fluctuations versus $1/T$. The value of D can be determined from eq 3.

q^* was set equal to the scattering vector $q_m(T_r)$ at the scattering maximum at a particular temperature T_r, much higher than the T_{ODT} of the block copolymer. Table 3 summarizes the values of q^* and, also, the values of T_r chosen for the seven SI diblock copolymers investigated in this study.

It should be mentioned that the Leibler theory,[19] which is based on the Landau-type mean-field theory, predicts that $1/I_m$ or $1/I(q^*)$ decreases linearly with $1/T$ in the *disordered* state, i.e.,

$$1/I_m \text{ or } 1/I(q^*) \sim a - b/T \tag{9}$$

where a and b are positive constants. Equation 9 assumes that the temperature dependence of the Flory−Huggins segmental interaction parameter between the block chains is given by

$$\chi = A + B/T \tag{10}$$

where A and B are constants. Further, the Leibler theory[19] predicts that D or q_m in disordered state is independent of temperature T, except for a small temperature variation, which originates from the temperature dependence of the radius of gyration of block copolymer chain $R_g(T)$, i.e.,

$$D/R_g(T) \text{ or } q_m R_g(T) \sim T^0 \tag{11}$$

Thus, in the context of the mean-field theory, the deviations in the temperature dependence of $1/I_m$ or $1/I(q^*)$ from eq 9, and the deviations in the temperature dependence of D from eq 11, are ascribed to an *onset* of the ordering process and hence may be utilized for determination of the T_{ODT} of a block copolymer. In this paper we will check the mean-field theory and deviations from the mean-field behavior due to *thermal concentration fluctuations*.[20]

For a block copolymer in the *disordered* state, $q_m(T_r)$ is nearly equal to $q_m(T)$ because $q_m(T)$ does not vary much with temperature (T). Therefore it is reasonable to expect that plots of $1/I_m$ versus $1/T$ would provide the same information as plots of $1/I(q^*)$ versus $1/T$. However in the *ordered* state of a block copolymer, $q_m(T)$ usually exhibits a shift (in fact, $q_m(T)$ decreases) with T, and the peak width also changes with T, making plots of $1/I(q^*)$ versus $1/T$ look quite different from plots of $1/I_m$ versus $1/T$, as will be shown below in Figures 3−6. This is simply because $1/I(q^*)$ is very sensitive to a *small shift* of $q_m(T)$ with increasing T, as compared to $1/I_m$. Thus, comparison of plots of $1/I_m$ versus $1/T$ with plots of $1/I(q^*)$ versus $1/T$ is very useful to judge whether a block copolymer under consideration is in the *ordered* state or the *disordered* state.

Plots of $1/I_m$ versus $1/T$, plots of $1/I(q^*)$ versus $1/T$, and plots of D versus $1/T$ are given in Figures 3−6 for some of the seven SI diblock copolymers synthesized in this study. In Figures 3 and 4 we observe a discontinuity in $1/I_m$ in the vicinity of a certain critical temperature for SI-Q and SI-S, as shown by the vertical broken lines, but *not* for SI-O and SI-L. In the beginning of this study, we were skeptical about the existence of discontinuity in the plot of $1/I_m$ versus $1/T$ and $1/I(q^*)$ versus $1/T$ at or near a certain critical temperature. However, after analyzing the high-temperature resolution SAXS data for SI-Z, SI-X, and SI-R, the results of which will be presented below, we have become convinced that the discontinuity in the plots of $1/I_m$ versus $1/T$ and $1/I(q^*)$

Table 3. Values of q* Used in the Plots of $1/I(q^*)$ versus $1/T$

sample code	q^* (nm^{-1})[a]	T_r (°C)
SI-Q	0.319	141
SI-Z	0.370	150
SI-S	0.418	140
SI-X	0.390	170
SI-R	0.445	157
SI-O	0.357	160
SI-L	0.260	210

[a] These values of q^* correspond to the scattering vector $q_m(T_r)$ at the scattering maximum at a particular temperature T_r indicated in this table. Note that the experimental values of q_m shift with temperature.

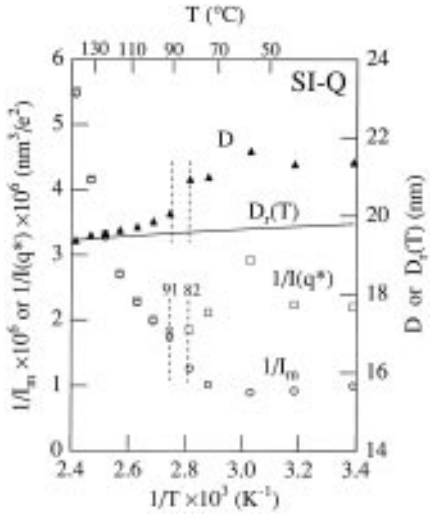

Figure 3. Plots of $1/I_m$ versus $1/T$ (○), $1/I(q^*)$ versus $1/T$ (□), D versus $1/T$ (▲), and $D_r(T)$ versus $1/T$ (—) for SI-Q. The numbers attached to the vertical broken lines hereafter indicate the temperatures (°C) in the interval of which ODT is expected to occur.

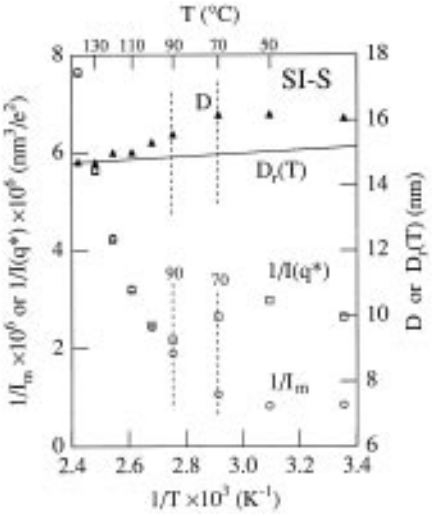

Figure 4. Plots of $1/I_m$ versus $1/T$ (○), $1/I(q^*)$ versus $1/T$ (□), D versus $1/T$ (▲), and $D_r(T)$ versus $1/T$ (—) for SI-S.

versus $1/T$, which are observed in Figures 3 and 4 for the block copolymers SI-Q and SI-S, is real. As a matter of fact, this observation was first noted by Bates et al.[21,22] and subsequently confirmed by Stühn et al.,[7] Wolff et al.,[8] Hashimoto et al.,[11] Floudas et al.,[23] and Sakamoto et al.[24]

In reference to Figures 5 and 6, we speculate that the absence of a discontinuity in $1/I_m$ in the vicinity of a certain critical temperature for SI-O and SI-L is attributable to the *kinetic effects*, as will be described immediately below. It should be remembered that both SI-O and SI-L have cylindrical microdomains of PI in PS matrix (see Table 1) and that they have molecular weights higher than the rest of the block copolymers (SI-Q, SI-Z, SI-S, SI-X, and SI-R). Also, the glass transition temperatures of the PS phase in SI-O and SI-L are much higher than those in the rest of the block copolymers (SI-Q, SI-Z, SI-S, SI-X, and SI-R).[12] It seems then reasonable to speculate that the ordering process into the hexagonally packed PI cylinders in the PS matrix for SI-O and SI-L would be much slower than the ordering process into the hexagonally packed PS cylinders in the PI matrix for SI-Q and SI-Z. Thus the

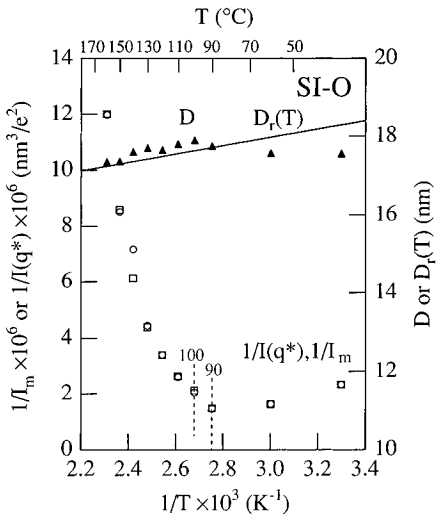

Figure 5. Plots of $1/I_m$ versus $1/T$ (○), $1/I(q^*)$ versus $1/T$ (□), D versus $1/T$ (▲), and $D_r(T)$ versus $1/T$ (—) for SI-O.

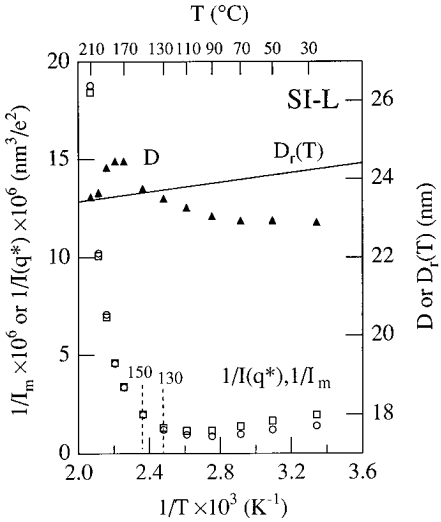

Figure 6. Plots of $1/I_m$ versus $1/T$ (○), $1/I(q^*)$ versus $1/T$ (□), D versus $1/T$ (▲), and $D_r(T)$ versus $1/T$ (—) for SI-L.

samples of SI-O and SI-L used in the SAXS experiments might have had a significant distortion in the long range order, which consequently obscured the existence of discontinuity in the plots of $1/I_m$ versus $1/T$ and $1/I(q^*)$ versus $1/T$ at or near a certain critical temperature. This subject deserves further investigation.

In reference to Figures 3 and 4, the upturn of $1/I(q^*)$ through the discontinuity with increasing $1/T$ (i.e., as the temperature decreases) reflects a shift of the peak scattering vector toward smaller values of q and hence an increase of D. The upturn thus clearly demonstrates an onset of the ordering process and the growth of the microdomains which invoke chain stretching.

It is of interest to observe in Figure 3 that in the plots of D versus $1/T$ for SI-Q, which has cylindrical microdomains of PS in PI matrix, the slope $dD/d(1/T)$ also shows a discontinuity at the same temperature interval where plots of $1/I_m$ versus $1/T$ show a discontinuity. The slope on the higher temperature side of ODT is always smaller than that on the lower temperature side. Note that the slope on the lower temperature side represents both the increase in order and the growth of microdomains as the temperature is decreased, and the slope on the higher temperature side represents a change in D in the disordered state. On the other hand, we observe in Figure 4 that a discontinuous change of slope

in the plot of D versus $1/T$ at or near a certain critical temperature is *not* conspicuous for SI-S which has bicontinuous microdomains. Earlier, similar observations[11,21,23,24] were noted for nearly symmetric block copolymers having lamellar microdomains. In Figures 5 and 6 a discontinuous change of slope in the plot of D versus $1/T$ at or near a certain critical temperature is *not* discernible for SI-O and SI-L. We already pointed out that the determination of T_{ODT} for SI-O and SI-L was very difficult, if not impossible, in the present study. A rather unusual temperature dependence of D, observed in Figure 5 for SI-O and in Figure 6 for SI-L, is attributable to a nonequilibrium effect in the change of the domain structure with temperature. In order to unambiguously determine the T_{ODT}s for SI-O and SI-L, we must begin with cylindrical microdomains with the long range order higher than the one used in the present study. This, however, would require a prolonged annealing at temperatures lower than the T_{ODT}.

It is worth noting in Figures 3−6 that the temperature dependence of D appears to level off as the temperature decreases below a certain critical value, say for $1/T \gtrsim 3.0 \times 10^{-3}$ K^{-1}. It turns out that the leveling off of D in the plots of D versus $1/T$ takes place at temperatures below the glass transition temperature of the PS phase ($T_{g,PS}$) in the SI diblock copolymers, the values of which are given in ref 12.

Let us now discuss the slope of the plots of D versus $1/T$ at temperatures above T_{ODT}. It is important to note that the slope of the D versus $1/T$ plot at the higher temperature side is definitely larger than that expected from the temperature dependence of the radius of gyration, $R_g(T)$, i.e.,

$$D_r(T) = [R_g(T)/R_g(T_r)]D(T_r) \qquad (12)$$

(solid line in Figures 3−6), where T_r is a reference temperature.[24] This implies that the scattering from this region cannot be strictly described by the mean-field theory.[19] The temperature range where the mean-field random phase approximation (RPA) theory is applicable may exist at even higher temperatures. Thus the disordered state attained in the present investigation for the seven SI diblock copolymers is, by and large, affected by thermal fluctuations and hence should be described in the context of non-mean-field theory.[20] The crossover temperature from the mean-field to non-mean-field disordered state[24] must exist at temperatures higher than those covered in the present investigation. Below we show this crossover for SI-X by adding a small amount of dioctylphthalate (DOP).

New Analysis of SAXS Profiles for Determination of T_{ODT}. Let us now use plots of the square of hwhm (σ_q^2) of the first-order scattering maximum versus $1/T$, which was first introduced by Stühn et al.[7] and Ehlich et al.,[13] to investigate the ODT of SI diblock copolymers. Such plots have a theoretical basis of mean-field theory (see Appendix). Figures 7 and 8 give plots of σ_q^2 versus $1/T$ for the seven SI diblock copolymers synthesized in this study. The general trend of the temperature dependence of σ_q^2 that can be observed in Figures 7 and 8 is very similar to that observed from the plots of $1/I_m$ versus $1/T$, given in Figures 3−6, namely, except for SI-O and SI-L, a discontinuity in σ_q^2 is seen in the vicinity of a certain critical temperature. Although there is no clear discontinuity in the plots of σ_q^2 versus $1/T$ and $1/I_m$ versus $1/T$ for SI-O and SI-L, from the changes of the temperature dependence of σ_q^2,

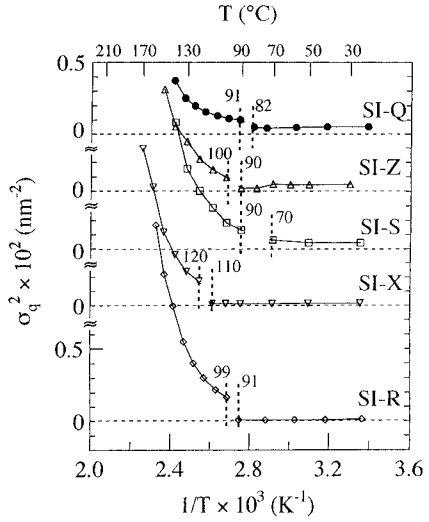

Figure 7. Plots of σ_q^2 versus $1/T$ for (●) SI-Q, (△) SI-Z, (□) SI-S, (▽) SI-X, and (◇) SI-R.

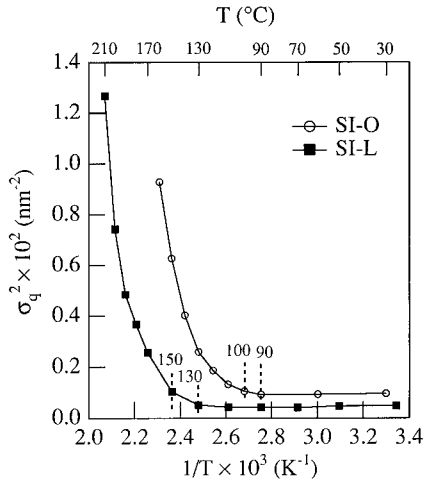

Figure 8. Plots of σ_q^2 versus $1/T$ for (○) SI-O and (□) SI-L.

$1/I_m$, and $1/I(q^*)$, we assign tentatively the T_{ODT} for SI-O to be 90−100 °C and the T_{ODT} for SI-L to be 130−150 °C because above these temperatures the values of σ_q^2, $1/I_m$, and $1/I(q^*)$ increase sharply. It should be mentioned that $1/I_m$ and σ_q^2 have the same physical meaning, but σ_q^2 is more sensitive and, also, more reliable than $1/I_m$. The sharpness of discontinuity in the plots of $1/I_m$ versus $1/T$ and σ_q^2 versus $1/T$ is described in the next section.

Analysis of ODT from High-Temperature Resolution SAXS Profiles. Having encountered some difficulties with determining accurate values of T_{ODT} from the SAXS profiles given in Figures 3−8, which were obtained with a temperature increment of ca. 10 °C or greater, we repeated SAXS experiments with a temperature increment of 1 or 2 °C. Naturally the thermal history of the specimen is different from that given in Table 2 for the conventional SAXS analysis.

Desmeared SAXS profiles for SI-X obtained from such experiments are given in Figure 9,[18] from which we observe a very sharp change in SAXS profile at a temperature between 111 and 112 °C, i.e., between profiles 2 and 3, which can reasonably be assumed to reflect ODT without further analyses using plots of $1/I_m$ versus $1/T$, $1/I(q^*)$ versus $1/T$, and σ_q^2 versus $1/T$. Figure 10 gives plots of $1/I_m$ versus $1/T$ and σ_q^2 versus $1/T$, for SI-X, showing a sharp discontinuous change at temperatures between 111 and 112 °C, i.e., at T_{ODT} =

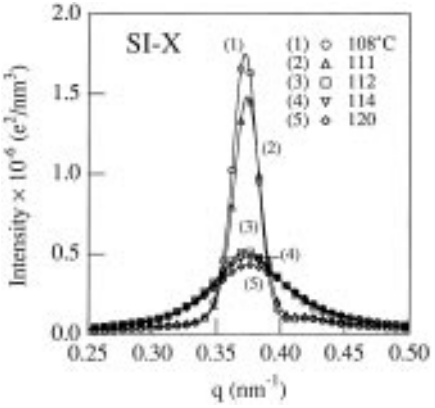

Figure 9. High-temperature resolution SAXS profiles for SI-X at various temperatures near the ODT: (1) 108, (2) 111, (3) 112, (4) 114, and (5) 120 °C.

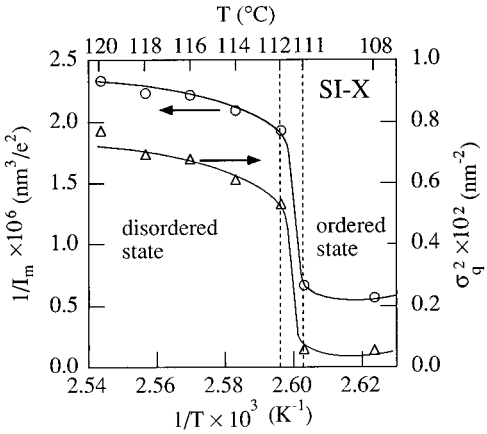

Figure 10. Temperature dependence of $1/I_m$ (○) and σ_q^2 (△) for SI-X near T_{ODT}.

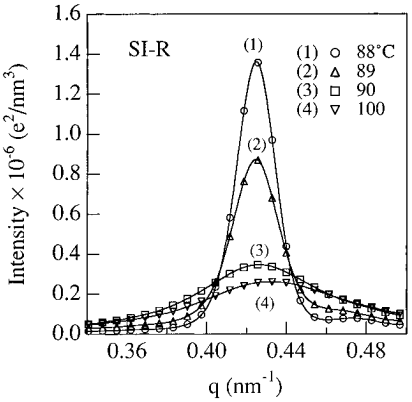

Figure 11. High-temperature resolution SAXS profiles for SI-R at various temperatures near the ODT: (1) 88, (2) 89, (3) 90, and (4) 100 °C.

111 ± 0.5 °C. Note that the previous high-temperature resolution analysis for SI-X was done on the smeared SAXS profiles (see Figures 5 and 6 of ref 11). Desmeared SAXS profiles obtained from SI-R with a temperature increment of 1 or 2 °C are given in Figure 11,[18] from which we observe a very sharp change in SAXS profile at a temperature between 89 and 90 °C, i.e., between profiles 2 and 3, which can reasonably be assumed to reflect ODT. Figure 12 gives plots of $1/I_m$ versus $1/T$ and σ_q^2 versus $1/T$, for SI-R, with each curve showing a sharp discontinuous change at temperatures between 89 and 90 °C, i.e., at $T_{ODT} = 89.5 \pm 0.5$ °C. From Figures 10 and 12 we can conclude that the measurements of the SAXS profiles at small tempera-

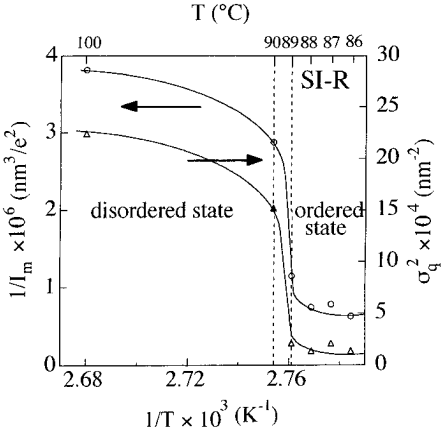

Figure 12. Temperature dependence of $1/I_m$ (○) and σ_q^2 (△) for SI-R near T_{ODT}.

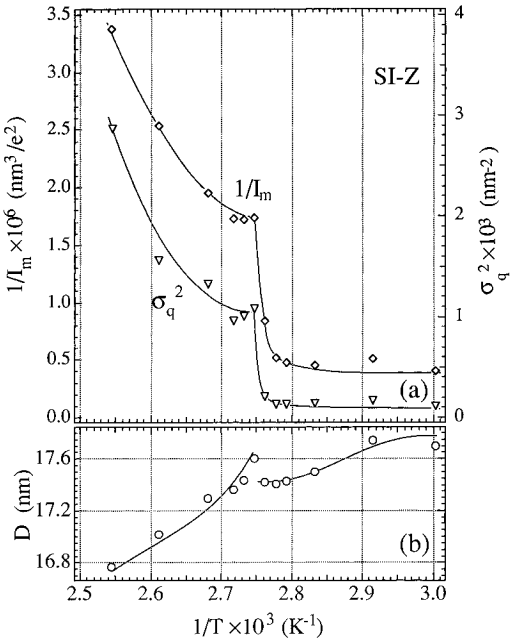

Figure 13. (a) Temperature dependence of $1/I_m$ (○) and σ_q^2 (△) for SI-Z near T_{ODT}. (b) Temperature dependence of D of SI-Z near T_{ODT}.

ture increments near ODT allow a precise determination of T_{ODT} with an accuracy to within 1 °C. The sharp discontinuous changes in the plots of σ_q^2 and $1/I_m$ observed in Figures 10 and 12 confirm the nature of ODT as being a *thermal-fluctuation-induced* first-order phase transition. It should be mentioned that we observe a relatively small change of D with T over a narrow range of temperatures covered for both SI-X and SI-R, simply because the segregation power, χN (N being the total degree of polymerization of the block copolymer), changes little with temperature.

Figure 13 shows high-temperature resolution SAXS results for SI-Z having cylindrical microdomains. Although not included in this paper, the desmeared SAXS profiles for SI-Z showed a discontinuous change in SAXS profile over a narrow range of temperatures between 89 and 91 °C, as found for SI-X (Figure 9) and SI-R (Figure 11). The results shown in Figure 13 indicate the presence of a sharp discontinuity in the plots of $1/I_m$ versus $1/T$ and σ_q^2 versus $1/T$, even for the block copolymer having cylindrical microdomains, enabling us to have an accurate determination of $T_{ODT} = 90 \pm 1$ °C.

Table 4. Comparison of the T_{ODT} Determined from SAXS with That Determined from a Rheological Method for the SI Diblock Copolymer Synthesized in This Study

	T_{ODT} (°C)		
sample code	SAXS	rheology[a]	morphology
SI-Q	82−91	95	PS cylinder
SI-Z	89−91[b]	90	PS cylinder
SI-S	70−90	80	bicontinuous
SI-X	111−112[b]	120	lamella
SI-R	89−90[b]	100	lamella
SI-O	90−100[c]	130	PI cylinder
SI-L	130−150[c]	170	PI cylinder

[a] Reference 12. [b] High-temperature resolution SAXS analysis. [c] No discontinuity in the plots of $1/I_m$, $1/I(q^*)$, and σ_q^2 versus $1/T$ was observed, and thus the T_{ODT} was determined to be the temperature above which the values of $1/I_m$, $1/I(q^*)$, and σ_q^2 increase sharply with temperature.

Comparison of SI-Z with SI-X or SI-R shows one striking difference in the temperature dependence of D. Specifically, in SI-Z, which forms cylindrical microdomains in the ordered state, D increases discontinuously upon raising the temperature across ODT (Figure 13b). Detailed interpretation of this discontinuity is beyond the scope of the present paper and deserves further investigation. However we tentatively suggest, as a possible model, a symmetry break from a superposition of plane wave fluctuations (in the *disordered* state) to hexagonal symmetry of the cylinders (in the *ordered* state). To the best of our knowledge, a discontinuous *increase* of D upon disordering has never been reported for SI and SB diblock copolymers. Note that Stühn et al.[7] reported a discontinuous *decrease* of D, contrary to our observation, upon ordering for an SI diblock copolymer forming lamellar microdomains. Using SI diblock copolymers forming lamellar microdomains, we have not been able to confirm the observation made by Stühn et al.[7] It should be mentioned that a discontinuous change of D, similar to that observed by us for SI-Z, was reported earlier by Floudas et al.[25] who employed a rather complicated block copolymer, referred to as 3-miktoarm star copolymer.

The sharp discontinuity observed in the temperature dependence of SAXS profiles and, also, in the plots of σ_q^2 versus $1/T$ and $1/I_m$ versus $1/T$, for SI-Z, SI-X, and SI-R, with high-temperature resolution experiments assures us that the discontinuous changes of the corresponding quantities observed with low-temperature resolution experiments are *real*. It is then reasonable to conclude that SI-Q and SI-S would also have discontinuous changes in the plots of σ_q^2 versus $1/T$ and $1/I_m$ versus $1/T$.

From the above discussion, it is worth making the following two remarks on identifying or investigating discontinuous changes in the SAXS data for SI-O and SI-L at ODT: (i) we must use the specimens having well-ordered microdomain structure as an initial condition, which would require a prolonged annealing in an *ordered* state, and (ii) we must employ a sufficiently slow heating or cooling rate.

The values of T_{ODT} determined in the present study, which employed SAXS, are summarized in Table 4 in which, for comparison, the values of T_{ODT} determined from rheological measurements[12] are also given. It can be seen in Table 4 that the values of T_{ODT} determined from SAXS measurements for the SI diblock copolymers, which exhibit a sharp discontinuity in the plots of $1/I_m$ versus $1/T$, $1/I(q^*)$ versus $1/T$, or σ_q^2 versus $1/T$, are about 10 °C lower than those determined from rheological measurements.

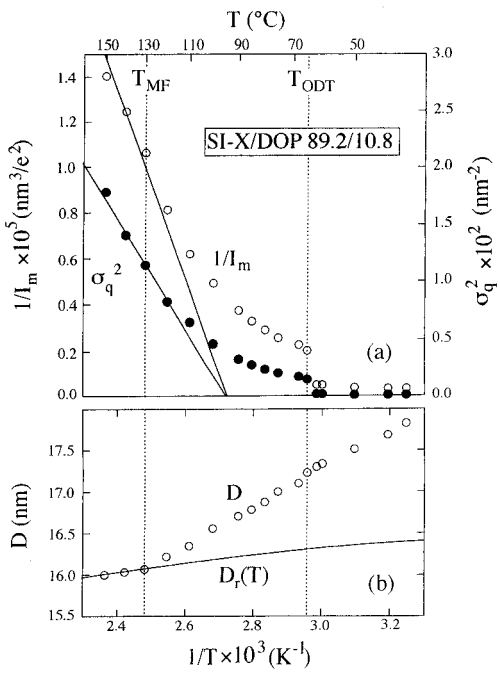

Figure 14. (a) Temperature dependence of $1/I_m$ (○) and σ_q^2 (△) for the 89.2/10.8 SI-X/DOP mixture near T_{ODT}. (b) Temperature dependence of D for the 89.2/10.8 SI-X/DOP mixture near T_{ODT}.

Crossover from Non-Mean-Field to Mean-Field Disordered State. We discuss here the crossover behavior in the *disordered* state, as seen in the plots of $1/I_m$ versus $1/T$, σ_q^2 versus $1/T$, and D versus $1/T$ for SI-X. To expand the temperature range where SI-X exists in the disordered state, we added a small amount of DOP (dioctyl phthalate) to SI-X in order to lower its T_{ODT} and expand the temperature range. Figure 14 shows plots of $1/I_m$ versus $1/T$, σ_q^2 versus $1/T$, and D versus $1/T$ for the SI-X/DOP system with the composition of 89.2/10.8 (by wt). In Figure 14 a discontinuity in the plots of I_m versus $1/T$ and σ_q^2 versus $1/T$ occurs at temperatures between 62 and 65 °C or for values of $1/T$ between 2.99×10^{-3} and 2.96×10^{-3} K^{-1} (see vertical broken lines). Thus the small amount of DOP added lowered the T_{ODT} by 48 °C and thus expanded the temperature range for the disordered state.

In Figure 14 we find that at temperatures sufficiently high (i.e., higher than $T_{MF} \cong 130$ °C indicated by a vertical line), the temperature dependence of D is *approximately* the same as that of $D_r(T)$ (see eq 12), in accord with the mean-field theory (see eq 11). At temperatures below T_{MF}, the temperature dependence of D is much larger than that of $D_r(T)$, implying a deviation from the mean-field theory. Here T_{MF} is defined by the temperature at which mean-field behavior crosses over non-mean-field behavior. At $T > T_{MF}$, both $1/I_m$ and σ_q^2 decrease with increasing $1/T$ *approximately* in accord with the mean-field theory (eqs 9 and A7). At $T < T_{MF}$, both $1/I_m$ and σ_q^2 have values which exceed those expected from the mean-field theory. This implies that at $T < T_{MF}$, the maximum scattered intensity (I_m) is lower than the mean-field value and the width of the scattering maximum (σ_q) is broader than the mean-field value. This indicates thermal fluctuation effects,[20] i.e., the thermal noise suppresses or washes out concentration fluctuations in the *disordered* state near ODT. The details of this crossover

behavior will be reported elsewhere.[24] The crossover behavior was also inferred in previous papers.[7,11,23]

Concluding Remarks

From the results presented above, we draw the following conclusions. (1) Except for SI-O and SI-L, all the low molecular weight SI diblock copolymers investigated in the present study exhibit clear discontinuities in the plots of σ_q^2 versus $1/T$ and $1/I_m$ versus $1/T$ at temperatures close to the ODT found by the rheological method. Thus we can conclude that the SAXS method itself can unequivocally determine T_{ODT}. Thus our results confirm the observation of the weak discontinuity of I_m^{-1} at T_{ODT} by Bates et al.[21] It should be noted that their SANS studies involve primarily PEP−PEE diblock copolymers which have lamellar microdomains in almost all cases and very high molecular weights, as compared to the SI diblock copolymer investigated in our study. Since the results of Bates et al. are not necessarily directly translatable to our low molecular weight SI diblock copolymers and for the copolymers having compositions biased from $f_{PS} \cong 0.5$, our results may offer a generalized view of the ODT phenomenon. (2) The high-temperature resolution SAXS experiments conducted in this study reveal that ODT is very sharp, occurring over the temperature range of ca. 1 °C for SI-X, SI-R, and SI-Z. Other SI diblock copolymers investigated in this study are also expected to have a sharp ODT. (3) The sharp discontinuities observed in the plots of σ_q^2 versus $1/T$ and $1/I_m$ versus $1/T$ support the prediction that ODT is a *fluctuation-induced first-order phase transition*. (4) The curvatures observed in the plots of σ_q^2 versus $1/T$ and $1/I_m$ versus $1/T$, on the higher temperature side of the ODT, where a block copolymer is in the *disordered* state, suggest that this state cannot be described by the mean-field RPA theory of Leibler.[19] This conclusion is also consistent with the experimental evidence that the temperature dependence of D is much greater than that predicted from the temperature dependence of $R_g(T)$. We speculate that the mean-field theory may be applicable at temperatures higher than that covered in the present SAXS experiments. (5) A possible reason why discontinuous changes in the plots of σ_q^2 versus $1/T$ and $1/I_m$ versus $1/T$, for SI-O and SI-L, were not observed at or near a certain critical temperature may lie in that *the ordering process* may take place very slowly in such block copolymers in which the microdomains of PI with a long range order are to be formed in the PS matrix which has a high glass transition temperature. Therefore it is reasonable to speculate that under an ordinary thermal treatment of specimen, the ordered state may have considerable defects, causing an increase of σ_q^2 and an increase of $1/I_m$, which will then decrease the extent of discontinuity in the plots of σ_q^2 versus $1/T$ and $1/I_m$ versus $1/T$ when the specimen is brought to a temperature above its T_{ODT}. (6) The curvatures in the plots of σ_q^2 versus $1/T$ and $1/I_m$ versus $1/T$ in the *disordered* state cannot be explained in terms of the 3-D kinetic Ising model, i.e., $(\sigma_q^2)^{1/\nu}$ and $(1/I_m)^{1/\nu}$ (with $\nu = 1.24$) do not show linear behavior with $1/T$. This may reflect the presence of thermal concentration fluctuations which belong to Brazovskii universality class, as proposed by Helfand and Fredrickson[20] and Bates et al.[21] and inferred by Leibler.[19]

Appendix

Below, we show that in the context of Landau-type mean-field theory, the square of hwhm (σ_q^2) is proportional to $1/T_s - 1/T$, where T_s is the mean-field spinodal temperature. Using a random phase approximation, Leibler[19] has shown that for an AB-type diblock copolymer the intensity, $I(q)$, in small-angle X-ray (or neutron) scattering is given by the following expression

$$I(q) \sim 1/[F(x)/N - 2\chi] \tag{A1}$$

where $x = (qR_g)^2$, χ is the Flory−Huggins interaction parameter, and $F(x)$ is given by eq IV-6 in ref 19. According to Leibler, the spinodal temperature (T_s) can be determined by $I_m \to \infty$, where I_m is $I(q)$ at $q = q^*$ or $x^* = (q^*R_g)^2$ and x^* (or q^*) is x (or q) that makes $I(q)$, defined by eq A1, a maximum. By expanding eq A1 around q^* or x^*, we obtain

$$I(q) \cong \frac{I(q^*)}{1 + (q - q^*)^2\xi^2} \tag{A2}$$

where ξ is the correlation length for thermal concentration fluctuations, and it is given by

$$\xi^2 = \frac{(\partial^2 F/\partial x^2)_{x^*}}{4(\chi_s - \chi)} \tag{A3}$$

If we define q_+ and q_- such that

$$\frac{1}{2}I(q^*) = \frac{I(q^*)}{1 + (q_\pm - q^*)^2\xi^2} \tag{A4}$$

then it follows that

$$(q_\pm - q^*)^2 = 1/\xi^2 \tag{A5}$$

Note that hwhm σ_q is given by

$$\sigma_q^2 = [(q_+ - q_-)/2]^2 \cong (q_+ - q^*)^2 \cong (q_- - q^*)^2 = 1/\xi^2 \tag{A6}$$

Thus use of eq A3 in eq A6 gives

$$\sigma_q^2 = \frac{1}{\xi^2} \sim \left|\frac{1}{T_s} - \frac{1}{T}\right|^{1/\nu} \tag{A7}$$

where ν is a critical exponent ($\nu = 1$ for mean-field theory and 1.24 for 3-D kinetic Ising model).

References and Notes

(1) Hashimoto, T. In *Thermoplastic Elastomers*; Legge, N. R., Holden, G., Schroeder, H. E., Eds.; Hanser: Munich, 1987; Chapter 12, Section 3, and references cited therein. The second edition is to appear in 1996.
(2) Bates, F. S.; Fredrickson, G. H. *Annu. Rev. Phys. Chem.* **1990**, *41*, 525 and references cited therein.
(3) Zin, W. C.; Roe, R. J. *Macromolecules* **1984**, *17*, 183.
(4) Mori, K.; Hasegawa, H.; Hashimoto, T. *Polym. J.* **1985**, *17*, 799.
(5) Owens, J. N.; Gancarz, I. S.; Koberstein, J. T.; Russell, T. P. *Macromolecules* **1989**, *22*, 3380.
(6) Holzer, B.; Lehmann, A.; Stühn, B.; Kowalski, M. *Polymer* **1991**, *32*, 1935.
(7) Stühn, B.; Mutter, R.; Albrecht, T. *Europhys. Lett.* **1992**, *18*, 427.
(8) Wolff, T.; Burger, C.; Ruland, W. *Macromolecules* **1993**, *26*, 1707.
(9) Sakurai, S.; Kawada, H.; Hashimoto, T.; Fetters, L. J. *Macromolecules* **1993**, *26*, 5796.
(10) Winey, K. I.; Gobran, D. S.; Xu, Z.; Fetters, L. J.; Thomas, E. L. *Macromolecules* **1994**, *27*, 2392.
(11) Hashimoto, T.; Ogawa, T.; Han, C. D. *J. Phys. Soc. Jpn.* **1994**, *63*, 2206.

(12) Han, C. D.; Baek, D. M.; Kim, J. K.; Ogawa, T.; Sakamoto, N.; Hashimoto, T. *Macromolecules* **1995**, *28*, 5043.
(13) Ehlich, D.; Takenaka, M.; Hashimoto, T. *Macromolecules* **1993**, *26*, 492.
(14) Kim, J. K.; Han, C. D. *Macromolecules* **1992**, *25*, 271.
(15) (a) Hashimoto, T.; Suehiro, S.; Shibayama, M.; Saijo, K.; Kawai, H. *Polym. J.* **1981**, *13*, 501. (b) Suehiro, S.; Saijo, K.; Ohta, Y.; Hashimoto, T.; Kawai, H. *Anal. Chim. Acta* **1986**, *189*, 41.
(16) Fujimura, M.; Hashimoto, T.; Kawai, H. *Mem. Fac. Eng., Kyoto Univ.* **1981**, *43* (2), 224.
(17) Hendricks, R. W. *J. Appl. Crystallogr.* **1972**, *5*, 315.
(18) A small peak existing just at the right-hand side foot of the first-order peak is an artifact due to our desmearing process, i.e., an instability of desmearing of the profile which is very sharp in the case when no smearing occurs.
(19) Leibler, L. *Macromolecules* **1980**, *13*, 1602.
(20) Fredrickson, G. H.; Helfand, E. *J. Chem. Phys.* **1987**, *87*, 697.
(21) Bates, F. S.; Rosedale, J. H.; Fredrickson, G. H. *J. Chem. Phys.* **1990**, *92*, 6255.
(22) Almdal, K.; Rosedale, J. H.; Bates, F. S.; Wignall, G. D.; Fredrickson, G. H. *Phys. Rev. Lett.* **1990**, *65*, 1112.
(23) Floudas, G.; Pakula, T.; Fischer, E. W.; Hadjichristidis, N.; Pispas, S. *Acta Polym.* **1994**, *45*, 176.
(24) Sakamoto, N.; Hashimoto, T. *Macromolecules* **1995**, *28*, 6825.
(25) Floudas, G.; Hadjichristidis, N.; Iatrou, H.; Pakula, T.; Fischer, E. W. *Macromolecules* **1994**, *27*, 7735.

MA951066V